energies

MDPI

Article

Performance Analysis of a Combined Solar-Assisted Heat Pump Heating System in Xi'an, China

Chao Huan [1,3], Shengteng Li [1,3], Fenghao Wang [2,*], Lang Liu [1,3,*], Yujiao Zhao [1,3], Zhihua Wang [2] and Pengfei Tao [4]

1 Energy School, Xi'an University of Science and Technology, Xi'an 710054, China
2 School of Human Settlements and Civil Engineering, Xi'an Jiaotong University, Xi'an 710049, China
3 Key Laboratory of Western Mines and Hazards Prevention, Ministry of Education of China, Xi'an 710054, China
4 Key Laboratory of Coal Resources Exploration and Comprehensive Utilization, Ministry of Land and Resources, Xi'an 710021, China
* Correspondence: fhwang@mail.xjtu.edu.cn (F.W.); liulang@xust.edu.cn (L.L.); Tel.: +86-13227006940 (F.W.); +86-15829310227 (L.L.)

Received: 27 May 2019; Accepted: 26 June 2019; Published: 29 June 2019

Abstract: This study proposed a combined solar-assisted heat pump (SAHP) system that could operate in the serial mode or parallel mode. For this proposed system, a stable year-round operation could be achieved without the assistance of electric heating or low-temperature heat pump. By analyzing the heat balance equations, a correlation of the combined SAHP system for the two modes switched was obtained, which provided a theoretical basis for the optimal operation of this system. In addition, the performance of the proposed system applied in a university bathroom in Xi'an district was investigated using TRNSYS. The results illustrated that compared to the serial and parallel systems, the proposed system exhibited a good performance on energy efficiency. The annual average coefficient of performance (COP) of the proposed system was 5.7, obviously higher than those of the serial system and the parallel system, which were 3.3 and 4.3, respectively. Therefore, the results in this study could provide the theoretical guidance and reference for practical engineering design.

Keywords: solar-assisted heat pump; combined system; serial system; parallel system; COP; TRNSYS

1. Introduction

At present, one third of the global energy consumption is used in the building sector [1,2], and nearly 40% of it is related to heating, ventilating and air conditioning (HVAC) systems [3]. The accelerated increase in fossil fuel cost has resulted in a high cost of the space heating in recent years [4]. Therefore, how to provide a clean and efficient building energy supply system has become a worldwide issue. Numerous studies have shown that the solar energy is abundant and freely available in nature as well as has higher output efficiency than other energy sources [5,6]. For example, with an approximate energy conservation rate of 75%, solar building has become one of the most important branches in green buildings [7]. Thus, the utilization of solar energy will be popularized to a high degree. Especially in areas with abundant annual solar radiation, it could be used as an important auxiliary energy.

Since Jordan and Threlkeld [8] proposed the concept that combines solar energy with a heat pump, many researchers have carried out investigation on various aspects, such as energy efficiency, parameters design, and the operation performance of the solar-assisted heat pump system (SAHP) [9–11]. Moreover, most SAHP systems are designed for building hot water supply. The SAHP water heater is different from conventional solar water heating system. It is a device based on reverse Carnot cycle, which uses the evaporator to absorb energy from solar, air and other low-grade heat sources,

and heats the domestic hot water through the condenser. On the one hand, the SAHP water heaters overcome many problems that exist in conventional solar domestic hot water systems, such as large initial investment of collectors and pipeline corrosion. On the other hand, this combination method improves the efficiency of the heat pump in cold winter condition and ensures a satisfactory hot water supply when the solar radiation is instable and at low density, which has a significant effect on building energy consumption. The solar energy is helpful to enhance the performance of the heat pump that runs in a low-temperature environment. Sun et al. [12] demonstrated a comparative study between a SAHP system and an air source heat pump (ASHP) system in different seasons, and the results showed that the SAHP system has a remarkable high performance on COP in winter condition compared to the ASHP system. Liu et al. [13] and Yang et al. [14] found the SAHP system could achieve a COP of 4.0, while the average COP of the ASHP was 3.0 [15].

According to the coupling mode of the solar collector and evaporator, the SAHP system can be classified into direct-expansion solar-assisted heat pump (DX-SAHP) and indirect-expansion solar-assisted heat pump (IDX-SAHP) by different connection types between the solar collector and heat pump [16]. DX-SAHP is a common and simple method that delivers the solar energy to the evaporator of the heat pump in a serial configuration to enhance the system performance [17]. The improved efficiency is achieved because the high evaporator temperature increases the COP of the heat pump [17–19]. However, with further study, researchers found that the DX-SAHP performances in different regions differ dramatically due to the influence of solar radiation, which is because the refrigerant directly flows inside the solar collector. The most important task for DX-SAHP is to guarantee its working efficiency and stability in different regions [20]. Consequently, the IDX-SAHP has gradually attracted wide attention from researchers [21]. The IDX-SAHP can be classified into three different categories: the serial system, parallel system and complex system, as shown in Figure 1. In the serial system, the solar collector and water source heat pump (WSHP) are connected in series [22], and the heat absorption of the heat pump evaporator is supplied by the solar collector, as shown in Figure 1a. The difference between the serial IDX-SAHP and DX-SAHP lies in the existence of the heat exchanger, which is usually a water tank. Due to this configuration, the serial IDX-SAHP is limited by the available energy from the collector. Figure 1b shows the configuration of the parallel IDX-SAHP system, in which the heat pump (ASHP) and solar collector are independent units and simultaneously support the system heating load. This configuration makes the parallel system exhibit a better performance under the condition of abundant solar radiation and ambient temperature. The great advantage of the parallel system is the heat pump could stop operating when the heat output of the solar collector meets the system heating demand. Moreover, the system control and connection of the parallel system is simple in comparison with the serial and complex systems. The complex system is similar to the serial system, but has two heat sources, including solar energy; furthermore, it can make them replenish each other (as shown in Figure 1c). The most applicable system is the parallel solution that accounts for 61% of the market [23]. For the cold conditions, the advantages of the serial systems are more obvious. This is because the solar collector serves as the heat source of the heat pump evaporator, providing a stable and relatively appropriate evaporation temperature for the WSHP. Consequently, the serial system shows a better performance. Huan et al. [24] comparatively investigated performances of the serial and parallel systems, and the result showed that the serial system has a higher COP than the parallel in winter. Bakirci [25] studied the serial system performance applied in Erzurum, Turkey, in which the experimental data were collected from January to June (the ambient temperature was between −10.8 °C and 14.6°C). The results showed that the average system COP was 2.9 and indicated the outdoor environment could affect the SAHP system selection and design. However, in the summer condition and transition season, the performance and the stability of the parallel system are better than those of the serial system, particularly with abundant solar radiation [26,27]. This is because the solar collector provides a large amount of heating load. Liang et al. [28] investigated the solar assisted air source heat pump with flexible operation control. The results showed that the COP of the heat pump unit was enhanced with the increase of the solar

radiation during the typical sunny day in the heating season. Considering the climate condition, e.g., in a cold environment, a low-temperature heat pump [29] or an auxiliary electric heater is usually employed in the serial or parallel system, which greatly increases the system cost.

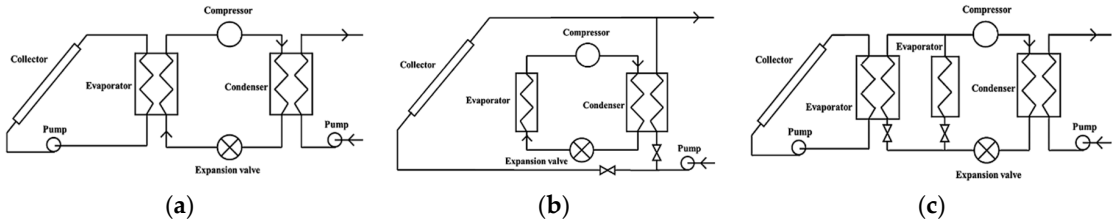

Figure 1. Sketch of the indirect-expansion solar-assisted heat pump (IDX-SAHP) system. (**a**) Serial system; (**b**) parallel system; (**c**) complex system.

Recently, there have been a series of performance optimization analyses on different types of SAHP systems. Due to the environmental condition and system matching relationship, the experimental results obtained in different areas are quite different [30–32]. In order to solve the problem that ensures the efficient operation of the SAHP system throughout the whole year, there are many optimization techniques for the system. Moreno-Rodríguez et al. [33] developed a mathematical model to optimize the DX-SAHP system by predicting the evaporation temperature and energy transmission. The system COP was between 1.7 and 2.9 for the load temperature of 51 °C. Banister et al. [34] built a dual tank SAHP system and compared it to a common serial system. Results indicated that the proposed system had a superior performance, which was able to maintain the hot water temperature at 53–57 °C during 99.9% of the year. Moreover, some studies have found that the optimized SAHP system could operate stably at night, under completely overcast conditions or in countries and regions that lack solar radiation [35,36]. However, how to realize a good combination of the serial system and the parallel system has not been fully discussed, by which the combined SAHP system could exhibit a high performance under different environment conditions. Based on a hot water supply system in a college bathroom in Xi'an district, this study proposed a combined SAHP system, which could be switched between the serial and parallel modes conveniently, and the water tank on the consumer side could be heated by optimal control, as shown in Figure 2. By analyzing the heat balance equations of system components and detailed TRNSYS simulations, the matching relationships between environmental conditions and system components, and the optimal operation for the combined SAHP system in Xi'an district were obtained.

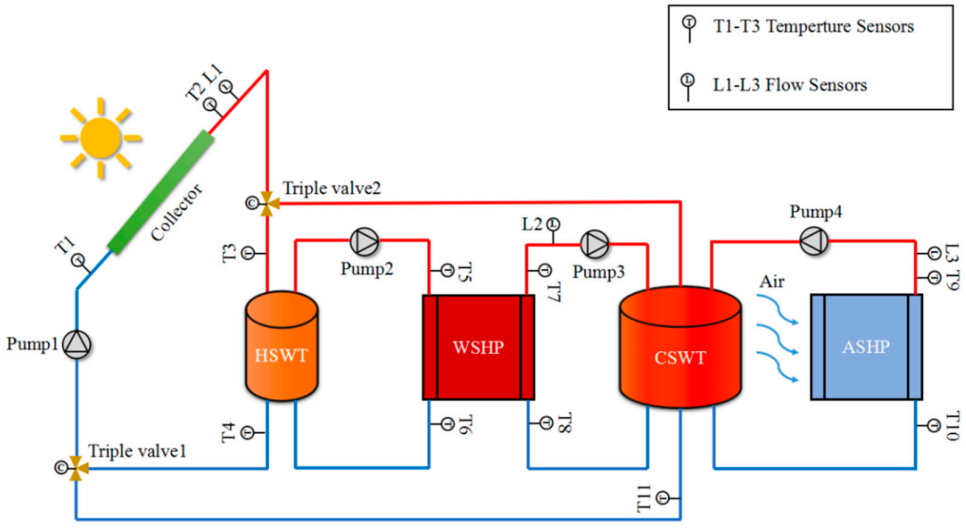

Figure 2. Schematic layout of the SAHP heating system.

2. Methodology

Simulation methods are commonly used in engineering research fields [37,38]. This study mainly focused on the high-efficiency operation of the combined system via mode switching. The performance of the system was investigated through TRNSYS simulation, and the validation experiment should be conducted to verify the simulation model [39,40].

2.1. System Descriptions

For this hot water supply system, 60 tons of water needed to be heated each day, with a target temperature of 50 °C. The working hours of this system was from 8:00 to 18:00, and the daily heating load was about 10^7 kJ. The proposed combined SAHP system could be switched between the serial and parallel modes conveniently. It was mainly composed of a solar collector, a heat storage water tank (HSWT), a WSHP, an ASHP and a consumer side water tank (CSWT), as shown in Figure 2. For the serial mode, the water stored in the HSWT was heated by the solar collector, which served as an evaporation heat source for the WSHP, finally, the water in the CSWT was heated by the WSHP until reaching the required temperature; for the parallel mode, the solar collector and the ASHP heated the water in the CSWT simultaneously. The system could achieve a steady and efficient operation throughout the whole year without electric auxiliary heat source.

2.2. Design Parameters of the Serial Mode

For Xi'an area, considering the frost issue, the evacuated collector was adopted [41]. In order to ensure the safe and stable operation of the system under the most disadvantageous outdoor climatic condition (such as bad weather conditions), the daily average solar radiation in the coldest month (January) was 9937 kJ·m^{-2}·d^{-1} according to the meteorological parameters of typical years in Xi'an, with a southern direction and a tilt angle of 59° [42]. According to the results found in previous research [43,44], the collector efficiency was 75%, and the heat coefficient of the heat pump was 2.8 [45,46]. Thus, if the daily heating load of the system (10^7 kJ) was needed, the daily heat-collecting capacity of the solar collector should be 6.42×10^6 kJ·d^{-1}. The area of the solar collector could be obtained using the following Equation [47]:

$$A_c = \frac{Q_u'}{I_c \eta_c}, \quad (1)$$

where Q_u' is the daily heat collection capacity of the solar collector, kJ·d^{-1}; I_c is the daily average solar radiation in the coldest month, kJ·m^{-2}·d^{-1}; and η_c is the collector efficiency.

The area of the collector was 860 m^2 by using Equation (1). The collector consisted of 60 sets of evacuated collectors of MK-58 × 1800-50-2 × 1-83-20, as shown in Figure 3. In view of the low-temperature environment, the antifreeze fluid mixed by alcohol and water (volume ratio of 1:2, freezing point of −14.2 °C) was used as the heating medium [48].

Figure 3. Evacuated collectors.

Considering the influence of the occupied area and the heat dissipation, a cylindrical accumulator was adopted as the HSWT [49]. The volume of the HSWT is given by Equation (2) [50,51], mainly affected by the property of the heating medium and the daily heat storage capacity.

$$V = \frac{Q_s'}{(\rho c)_w \Delta t (1 - \eta_s)}, \quad (2)$$

where Q_s' is the daily heat storage capacity, kJ·d^{-1}; $(\rho c)_w$ is the volumetric heat capacity of the heating medium, kJ·m^{-3}·°C^{-1}; Δt is the temperature difference of the heating medium, °C; and η_s is the heat loss rate of heating medium.

According to the typical meteorological parameters during January, it was supposed that during approximately two-thirds of the daytime, there was sufficient solar radiation, thus during another third of the daytime, the heat needed by the WSHP evaporation should be supplied by the HSWT. Consequently, the daily heat storage capacity was obtained to be 2.2×10^6 kJ·d^{-1} with consideration of an extra coefficient of 20%. Generally, the temperature difference of the heating medium was 10–15 °C [48], and it was supposed to be 12 °C in this study. Furthermore, the heat loss rate of the heating medium was generally 20%–40% [52], and it was supposed to be 20% due to the low working temperature of the HSWT in the serial mode. Finally, using Equation (2) the volume of the HSWT was found to be 55 m^3. Considering the economy and durability of the tank, the main structure of the tank was welded with a 3-mm-thick steel plate; the shell of the tank was composed of a 1.2 mm thick steel plate; and the whole water tank was thickened with a 200 mm insulation layer.

For the serial mode, the daily heat supply of the system was provided by the WSHP, with a value of 10^7 kJ and a running period of 10 h. Therefore, the heating power of the WSHP was 278 kW. According to the capacity of the heat pump and the working range of the evaporation, two RW210-F WSHPs were adopted, each with an input power of 48 kW and a circulating water flow of 20 T·h^{-1}.

2.3. Design Parameters of Parallel Mode

Due to the low-ambient temperature in winter conditions, the efficiencies of both the ASHP and solar collectors were at low level. Considering a certain heating load and the system stability, the heat pump should be selected according to the minimum monthly average temperature. In this study, the minimum monthly average temperature in Xi'an was −3 °C [42], and the heating power was 278 kW; thus, five DKFXRS-64II ASHPs were selected, each with an input power of 19 kW and a circulating water flow of 12 T·h^{-1}, as shown in Figure 4.

Figure 4. Air source heat pumps.

By studying the relationship between the collector area and the system initial investment of a parallel SAHP system in different months, Jiang et al. [53] found that the collector area could be designed according to the typical daily average radiation during the transition season. For Xi'an region, the typical daily average radiation is 15,000 kJ·m^{-2}·d^{-1} [42], consequently, the collector area was 1025 m^2 using Equation (1). However, the serial and parallel modes shared the same solar collector, given the investment [14], and the collector area was designed to be 860 m^2 in this experiment.

2.4. Measurement Instrumentation

In this experiment, a copper-constantan (T-type) was adopted as the temperature sensors. The total solar radiation projected onto the collector was measured by TBQ-2 pyranometer, with a sensitivity of 7~14 μV·W^{-1}·m^{-2}, a response time of less than 30 s, and a measurement range of 0~2000 W·m^{-2}. The installation angle of the pyranometer was consistent with the angle of the solar collector. Moreover, two layers of quartz glass cover made by optical cold processing were employed to reduce the influence of environmental changes on equipment performance. The water flow rate was measured by the YB-70H hand-held ultrasonic flowmeter. The measurement range for velocity was 0–30 m·s^{-1} and the applicable diameter range was 10–6000 mm. The real-time experimental data was recorded by a HP34970A data collector. The measuring instruments are shown in Figure 5. During the experimental process, the accuracy of measuring instruments was the main factor that caused system error [54,55]. In this study, the uncertainty analysis method put forward by Moffat was adopted [56]. Assuming the variant R, which is calculated from a set of independent variants $X_1, X_2, \ldots, X_n$, that is to say $R = R(X_1, X_2, \ldots, X_n)$, the uncertainty of the variant R can be determined by combining the uncertainties of individual terms and can be expressed as follows:

$$\delta R = \left[\sum_{i=1}^{n} \left(\frac{\partial R}{\partial X_i} \delta X_i \right)^2 \right]^{\frac{1}{2}}, \quad (3)$$

where δR is the total uncertainty of the experimental result R and δXi is the uncertainty of the independent variant Xi. The water temperature is a directly measured variable, thus the uncertainty of a measurement result was determined by the standard deviation of the arithmetic average value of the records. Thus, the maximum measurement uncertainty for water temperature was found to be 2.2%.

Figure 5. Measuring instruments. (**A**) HP34970A data collector; (**B**) TBQ-2 pyranometer; (**C**) YB-70H hand-held ultrasonic flowmeter; (**D**) DF-type centralized electric energy meter.

3. Modelling

TRNSYS is widely used for transient energy consumption calculation in complicated systems [57–59]. In this study, the TRNSYS software was adopted to investigate the system running efficiency and energy consumption under the serial and parallel modes, by which the optimal conditions of the mode switching for SAHP system could be obtained.

3.1. Models of the Two Modes

The main component modules (types) used in the simulation are summarized in Table 1. The evacuated collector and heat pumps modules needed to run with the user's source files while other modules only needed the corresponding input and output parameters. According to the modified coefficients of the two-dimensional incident angle [60] in Xi'an, the parameters of the evacuated collector were corrected. For the heat pump, the COP was influenced by the evaporation and condensation temperatures. The input file of the heat pumps was established by referring the heat pump performance curves provided by manufacturers.

Table 1. Main components used in the TRNSYS simulation.

Component	TRNSYS Type
Weather data reader	109
Evacuated collector	538
Controller	2
HSWT	4
CSWT	4
WSHP	668
Water pump	114
Load profile	14
Results	24
Printer	25
Graphic plotter	65
ASHP	941
Mixer	11

Figure S1 shows the TRNSYS model of the combined SAHP system. In this model, the most important Type was Equation, which controlled the operation mode of the proposed combined system, ensuring the efficient year-round operation of the system. When the combined system operated in the serial mode, the meteorological parameters of Xi'an were loaded at first by Type 109 and then transmitted to the evacuated collector (Type 538) as the input environmental parameters. The HSWT acted as the heat source for the WSHP (Type 668). The heating period of the WSHP was controlled

by the time controller. Water with an initial temperature of 10 °C was poured into the CSWT before 8:00 by a load profile and then was heated. Simultaneously, the on-off of the system was realized by a temperature controller (Type 2b). The logic diagram of the CSWT is shown in Figure 6. Once the water temperature in the CSWT reached 50 °C, the whole system was stopped. The main difference between the parallel and serial modes was that in the parallel mode, the meteorological data was loaded by Type 109 and then simultaneously transmitted to the evacuated collector (Type 538) and the ASHP (Type 941). When the combined system operated in the parallel mode, the ASHP and the collector heated the water in the CSWT (Type 4) separately. The energy consumptions and COP of the two systems were calculated by the integrator (Type 24). Finally, the performance results could be displayed on Graphic plotter (Type 65) or exported to a file.

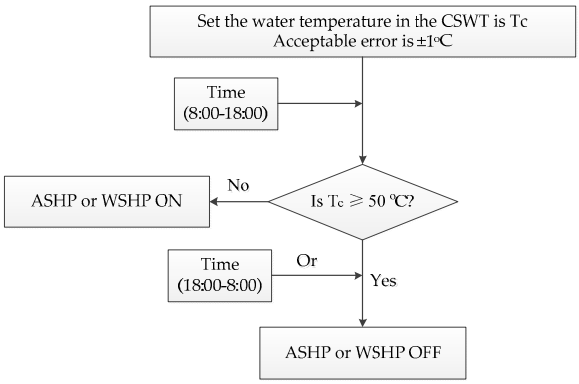

Figure 6. Logical diagram of the operation control for heat pump.

3.2. Model Validation

In this study, modules of the WSHP, ASHP, and evacuated collector were validated by the experiment, respectively. A total of 60 tons of cold water (10 °C) were filled into the CSWT before 8:00 and then heated by each validated module, with an objective temperature of 50 °C. The measured and simulated water temperatures in the CSWT during the heating process were compared. For the solar collector, the validation experiment was conducted on January 7–9. Figure 7a shows the measured and simulated water temperatures in the solar collector. It was found that a generally good agreement between the measured and simulated results could be achieved. For most cases, the relative error was around 10.2%. The maximal relative error was 14.8%, appearing at 8:00 in the second day, which is at the stage of daily heating period. This was because the high-temperature heat medium remaining from the previous day made the experimental value increase first, and then decrease. The validation experiment of the WSHP module was conducted on January 10–12. Two WSHPs simultaneously heated the water in the CSWT. Figure 7b shows the good agreement between the simulation and experimental results. The maximum error between the simulation and the measurement was 8.6%. The validation experiment of the ASHP module was carried out on February 18–20. Five ASHPs simultaneously heated the water in the CSWT. Figure 7c indicates that the experimental data fitted well with the simulation result, with a maximal error of 7.8%. For each day, the measured water temperature values were slightly lower than the simulated results. It was probably attributed to the direction and location of the ASHPs, where the ASHPs were sheltered by the buildings and therefore the actual ambient temperature around the ASHPs was lower than the input value of the simulation. Based on the validation of the aforementioned modules, the switching conditions of the system could be analyzed.

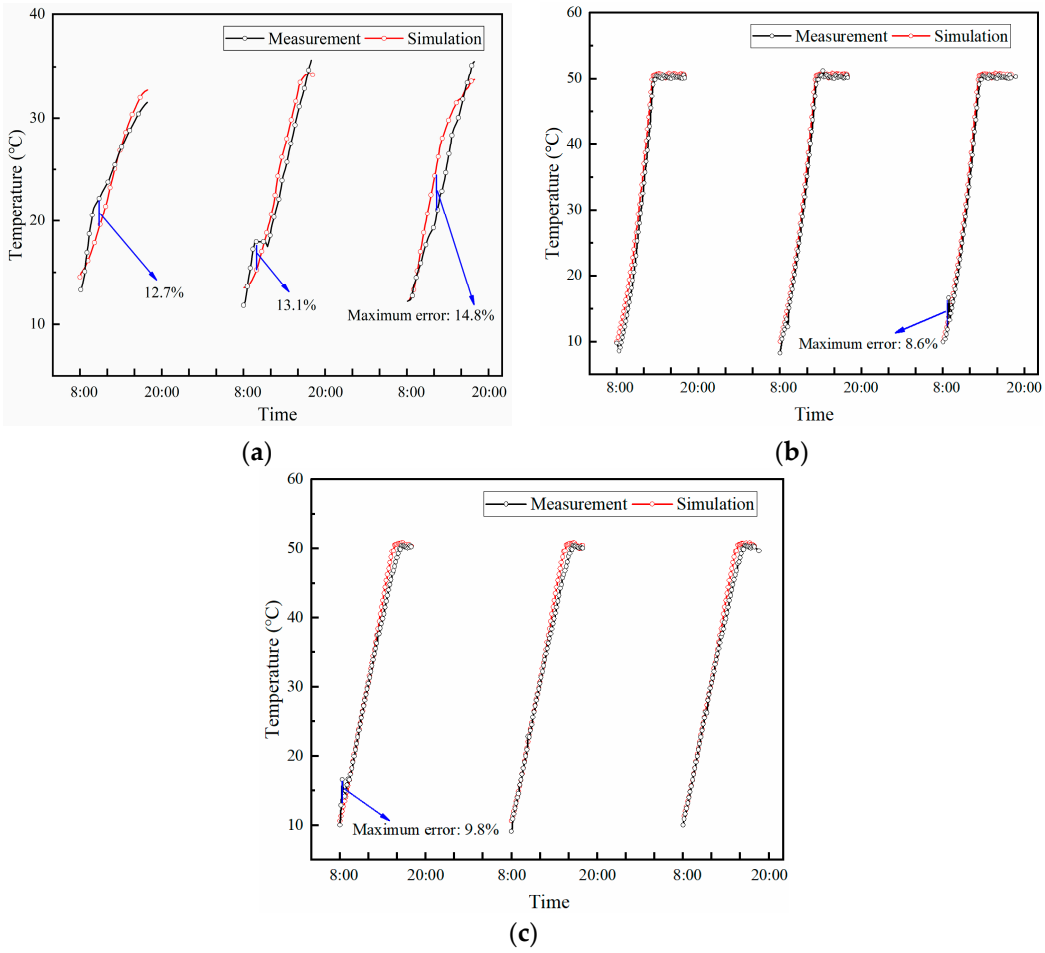

Figure 7. Water temperature changes; (**a**) validation of the evacuated collector; (**b**) validation of the water source heat pump (WSHP); (**c**) validation of the air source heat pump (ASHP).

4. Results and Discussions

4.1. Switching Analysis

The parallel mode had a high COP value during summer conditions because of the abundant solar radiation, which provided plenty of heat to the system. In contrast, the advantages of the serial mode were more obvious during winter conditions, due to the insufficient solar radiation and low-temperature environment. For most regions in northern China, there is a relatively large difference of outdoor weather parameters between sunrise and noon during a day, particularly in winter or transition season. Therefore, in different time periods during a day, we supposed that there might be different optimal operation mode of the SAHP system corresponding to different weather parameters.

In order to illustrate the rationality of this assumption, the comparative analysis was conducted in this study, which aimed to demonstrate the performance difference of the SAHP system with and without mode switching during a day. In view of the low temperature and weak solar radiation in the morning, the proposed combined system was started in the serial mode (at 8:00 each day), and was switched to the parallel mode at noon, when both the solar radiation and the ambient temperature are increased. According to the weather condition, the maximum ambient temperature and maximum solar radiation generally occurred at 12:00, thus 12:00 was supposed to be the mode switching time during a day for the preliminary assessment. The meteorological parameters are shown in Figure 8. In addition, the performance parameters of SAHP systems with and without mode switching are listed in Table 2, by which it was found that on April 1, the maximum solar radiation (I_m) was 3070 kJ·m^{-2}·h^{-1}, and the maximum ambient temperature (T_m) was above 14 °C. In this case, the COP of the parallel

mode was 8.84, while that of the serial mode was 4.06. However, as the solar radiation decreases, the efficiency of the collector will decrease dramatically, which led to the decline of COP in parallel mode. For March 21, when I_m was 1756 kJ·m^{-2}·h^{-1} and Tm was 13 °C, the COPs of the serial and parallel modes were 3.99 and 4.32, respectively; for March 1, when I_m was 2056 kJ·m^{-2}·h^{-1} and T_m was 11 °C, the COP of the serial mode was 3.94 and that of the parallel mode was 3.86. From these two results, it could be seen that the COPs of the two modes were simultaneously influenced by the solar radiation and ambient temperature. In addition, it was found that in the winter condition (January 11), the serial mode had a better performance than the parallel mode; with the increased ambient temperature and solar radiation, the parallel mode exhibited a performance advantage in transition season (March 21 and April 1). The comparison results fully illustrated the rationality and necessity of the mode switching during a day. However, to obtain the reasonable optimization method as well as the accurate results, the mode switching condition needed to be further analyzed by establishing heat balance equations of the SAHP system, which are detailed and discussed in Sections 4.2–4.4 in this manuscript.

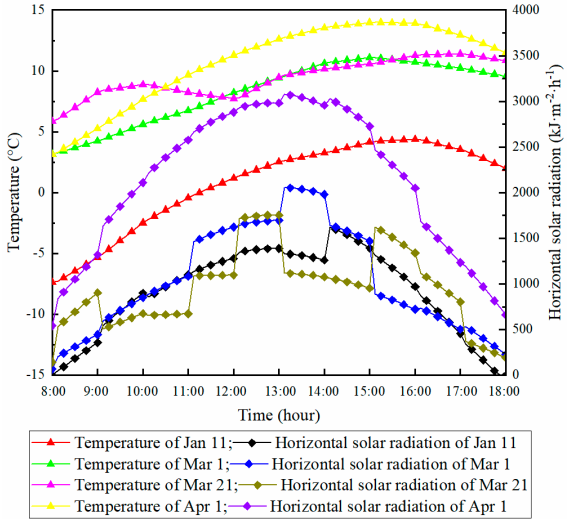

Figure 8. Meteorological parameters of the typical days.

Table 2. Performance comparison of the combined SAHP system with and without mode switching.

Performance Parameters	Jan 11			Mar 1			Mar 21			Apr 1		
	S Mode	S + P Mode		S Mode	S + P Mode		S Mode	S + P Mode		S Mode	S + P Mode	
		C	A		C	A		C	A		C	A
Heating capacity/10^6 kJ (C&A)	4.08	1.55	2.70	5.22	2.14	3.17	5.34	2.36	3.71	5.46	4.45	1.93
Energy consumption/10^6 kJ	1.26	1.35		1.32	1.38		1.34	1.40		1.35	0.72	
COP	3.24	3.15		3.94	3.86		3.99	4.32		4.06	8.84	

(C and A respectively represent the heat provided by the collector and the ASHP in parallel mode; S mode represents the serial mode (without mode switching); S + P mode represents the serial + parallel mode (with mode switching))

4.2. Heat Balance Equations of the SAHP System

To investigate the switching condition of working modes for the SAHP system, the heat balance of the system was examined. Based on the following assumptions, the heat balance equations of the SAHP system could be established:

(1) Stable operation of the system.
(2) Linear distribution of the temperatures in the solar collector and the heat exchanger.
(3) Negligible heat loss of pipes and valves.

For the parallel mode, the heat balance of the solar collector was described by Equation (4).

$$\overline{Q_u} = mC_p(T_{co} - T_{ci}) = F_r A[I/3600(\tau\alpha) - K_1(T_{ca} - T_a)], \quad (4)$$

where $\overline{Q_u}$ is the heat collection capacity of the solar collector, kw; mC_p is the heat capacity of the heating medium, kJ·°C^{-1}·s^{-1}; T_{co} is the outlet temperature of the collector, °C; T_{ci} is the inlet temperature of the collector, °C; T_{ca} is the average temperature of the collector, °C; F_r is the heat removal factor; A_c is the solar collector area, m^2; I is the solar radiation, kJ·m^{-2}·h^{-1}; $\tau\alpha$ is the product of the transmittance and absorption rates of the plate; K_1 is the heat transfer coefficient of the plate to environment, kW·m^{-2}·°C^{-1}; and T_a is the ambient temperature, °C.

The heat balance equation of the ASHP was

$$\overline{Q_k} = COP_a \cdot \overline{W} = \overline{Q_c} + \overline{W}, \quad (5)$$

where $\overline{Q_k}$ is the heat transfer capacity of the ASHP condenser, kw; *COPa* is the COP of the ASHP; $\overline{W}$ is the compressor power consumption of the ASHP, kw; $\overline{Q_c}$ is the heat transfer rate of the ASHP evaporator, kw.

For the parallel mode, the heat balance equation of the CSWT was defined as:

$$\overline{Q} = \overline{Q_u} + \overline{Q_k}, \quad (6)$$

where $\overline{Q}$ is the heating capacity of the CSWT under the parallel mode, kw.

For the serial mode, the heat balance equation of the solar collector was expressed as:

$$Q_u = mC_p(T_{co} - T_{ci}) = F_r A[I(\tau\alpha) - K_1(T_{ca} - T_a)], \quad (7)$$

where Q_u is the heat collection capacity of the solar collector, kw.

The heat balance equations of the HSWT were written as follows:

$$Q_s = Q_u - Q_c, \quad (8)$$

$$Q_s = K_s A_s(T_{sm} - T_a) + (mC_p)_s(\delta T_s/\delta\tau), \quad (9)$$

where Q_s is the heating capacity of the HSWT, kw; Q_c is the heat transfer rate of the WSHP evaporator, kw; K_s is the heat transfer coefficient of the HSWT, kW·m^{-2}·°C^{-1}; A_s is the heat exchange area of the HSWT, m^2; T_{sm} is the average water temperature in the HSWT, °C; $(mC_p)_s$ is the heat capacity of water, kJ·°C^{-1}·s^{-1}; $\delta T_s/\delta\tau$ is the water temperature change rate, °C.

The heat balance equation of the WSHP was:

$$Q_k = COP_s \cdot W = Q_c + W, \quad (10)$$

where Q_k is the heat transfer rate of the WSHP condenser, kw; COP_s is the COP of the WSHP; W is the compressor power consumption of the WSHP, kw.

For the serial mode, the heat balance equation of the CSWT was:

$$Q = Q_k, \quad (11)$$

where Q is the heating capacity of the CSWT under the serial mode, kw.

To analyze the switching conditions, other assumptions about heat transfer must be made:

(1) The compressor power consumption under the two modes was equal, which was described as follows:

$$W = \overline{W}. \tag{12}$$

(2) The condensation temperatures of the ASHP and WSHP were approximately the same at the mode switching timing, thus it was supposed that the COPs of the heat pump systems were only influenced by the evaporation temperature.

(3) The HSWT was insulated, thus the heat loss of the HSWT, e.g., $K_s A_s (T_{sm} - T_a)$ could be ignored.

According to previous studies on the performance of the ASHP and WSHP [61] as well as the parameters provided by the manufacturers, the relationship between the COP and the ambient temperature and that between the COP and the evaporation temperature could be obtained, as shown in Figure 9.

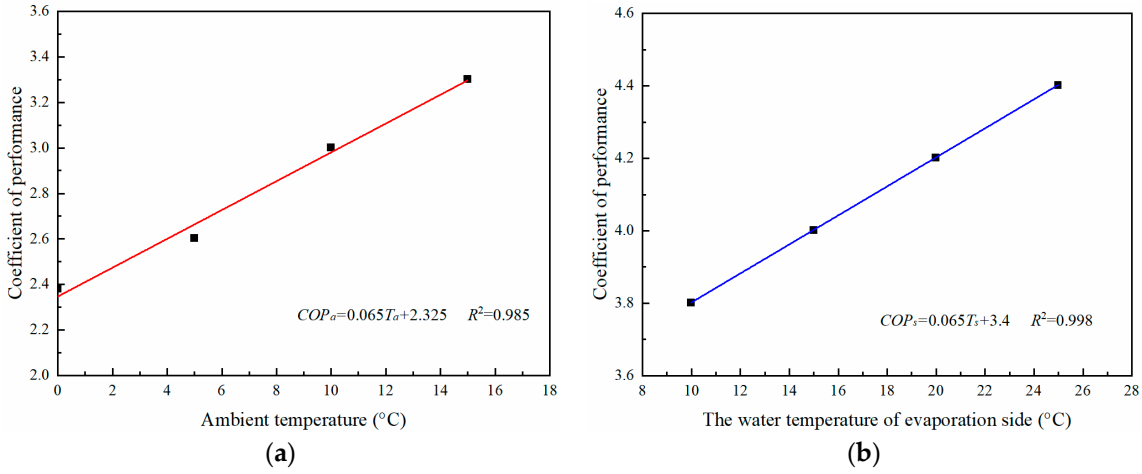

Figure 9. Performance curves of the heat pumps. (**a**) Performance curve of the ASHP; (**b**) performance curves of the WSHP.

Through linear fitting, the COPs of heat pumps could be expressed as follows:

$$COP_a = 0.065T_a + 2.325, \tag{13}$$

$$COP_s = 0.04T_s + 3.4, \tag{14}$$

where T_s is the water temperature in the HSWT, °C.

Given the results found by Zhang et al. [62], the value of F_r, $\tau\alpha$, and K_1 in Equations (3) and (6) were 0.6, 0.76, and 0.001, respectively, in this study. The constraint condition for mode switching was:

$$Q - \overline{Q} = 0. \tag{15}$$

Substituting Equations (4)–(6), and (10)–(14) into Equation (15) yields the following equation:

$$0.04T_s - 0.065T_a - 0.456\frac{AI}{W} + 1.075 = 0. \tag{16}$$

Similarly, substituting Equations (7), (9), (10) and (14) into Equation (8), we can obtain Equation (16).

$$(\delta T_s/\delta\tau) + 9.52 \times 10^{-6}\frac{W}{V}T_s + 5.71 \times 10^{-4}\frac{W}{V} = 1.64 \times 10^{-4}\frac{A}{V}I. \tag{17}$$

From Equations (16) and (17), it was found that when the compressor power consumption, solar collector area, and the volume of the HSWT are constant, the switching conditions are related to the water temperature in the HSWT (T_s) as well as the ambient temperature (T_a) and the solar radiation (I). The relationship between the water temperature in the HSWT and system running time can be illustrated by Equation (17).

4.3. Switching Conditions

For the combined solar-assisted heat pump proposed in this study, the solar collector area was 860 m^2, the compressor power was about 100 kW, and the volume of HSWT was 55 m^3. In addition, at the moment of mode switch, substituting the values of these parameters into Equation (16), it can be simplified as follows:

$$0.04T_s - 0.065T_a - 0.00109I + 1.075 = 0. \quad (18)$$

From Equation (18) it can be found that the mode switching conditions are mainly related to the ambient temperature and solar radiation. When the value of the left side of Equation (18) is above zero (as shown in Equation (19)), which indicated that the performance of the serial mode is higher than that of the parallel mode, the combined SAHP system should be switched to the parallel mode.

$$0.04T_s - 0.065T_a - 0.00109I + 1.075 > 0. \quad (19)$$

Considering that T_s was variable, the combined SAHP should be started in the serial mode for conveniently monitoring the value of T_s in real-time. As the ambient temperature and solar radiation were increasing gradually after 8:00 AM, the system would switch from the serial mode to the parallel mode at a proper time. Similarly, the parallel mode should be switched to the serial when its performance was worse than the serial system. The logic diagram of the mode switching is shown in Figure 10. The system loaded the real time values of T_a, I and T_s at first and transmitted them to Equation (19) to determine whether to switch to the parallel mode. According to the above analyses, it was obvious that the parallel mode would performance better if Equation (19) is below or equal to zero. However, the monitoring was still continuing. When the ambient temperature and solar radiation reduced to a certain extent, it would result in a low evaporation temperature of ASHPs and a limited solar heat output for the parallel system. In this case, the serial mode might perform better than the parallel mode, thus the system should be switched back to the serial mode. Therefore, the mode switching is a continuous cycle until 18:00 PM in each day.

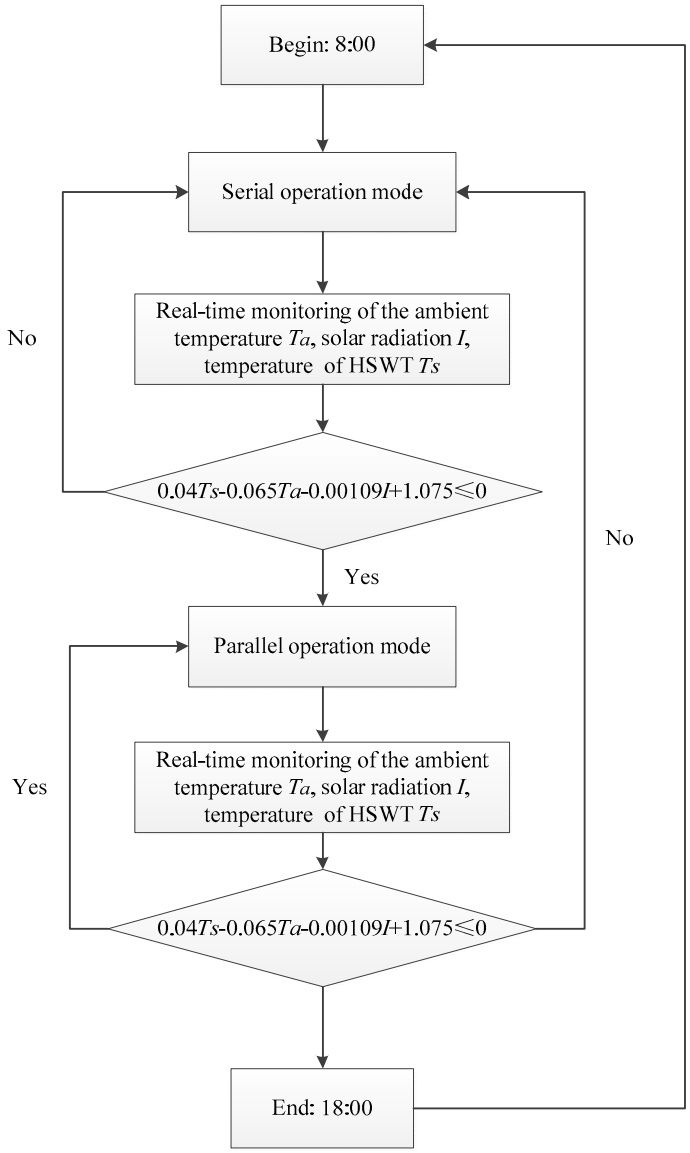

Figure 10. The logic diagram of the mode switching.

4.4. Annual Performance Analysis

Figure 11 shows the COP variations of the three systems. It could be found that in summer and transition season (1416–8016 h), the COP of the parallel mode was much higher than that of the serial mode, while in winter (0–1416 h and 8016–8760 h) the serial mode had a higher COP (compared to the parallel mode), which was in accordance with the previous studies [12,14]. The annual average COPs of the serial and parallel systems were 3.3 and 4.3, respectively. The combined SAHP system integrates both advantages of the serial and parallel systems. In winter condition, the COP of the combined SAHP system showed a higher COP than the serial system. This is owing to the relative strong solar radiation and high ambient temperature that occurred in the afternoon during the winter days, ensuring an appropriate operation condition for the parallel mode, in which the solar collector and the ASHP simultaneously provide the system heating load. Simultaneously, energy consumption of the collector system was much lower than that of heat pumps. In the transition season and summer condition, there was no significant difference between the COP values of the combined SAHP system and the parallel system. That meant, in most cases, the combined SAHP was operated under the parallel mode. In general, the combined SAHP system had an annual average COP of 5.7, which was

higher than those of the serial and parallel systems, indicating that the mode switching is an effective approach to improve the performance of heat pump system.

In addition, Figure 12 shows the heating capacity and energy consumption of the three different systems: the serial, parallel, and the proposed combined systems. It was found that for annual operation, the energy consumption of the combined SAHP system was 0.68×10^3 GJ, which was obviously lower than those of the serial and the parallel systems, with values of 1.17×10^3 GJ and 0.87×10^3 GJ, respectively, indicating the good energy efficiency of the combined SAHP system.

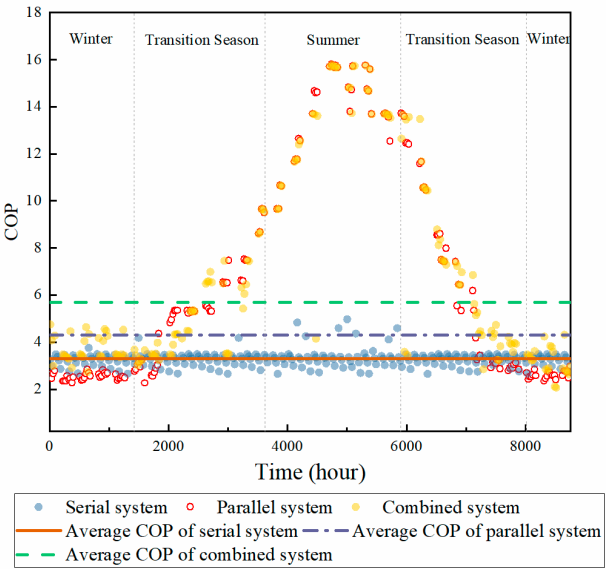

Figure 11. COP variations of the three systems during a whole year.

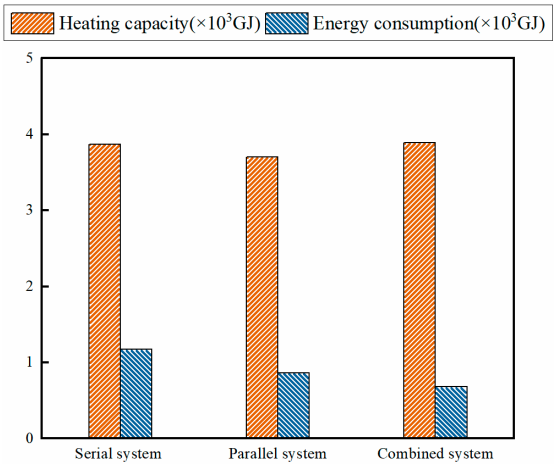

Figure 12. Annual performance of the three systems.

4.5. System Benefit Analysis

The annual energy-saving amount and the annual cost-saving amount of a system are often used as indicators for the benefit analysis of a solar heating system [63]. The annual energy-saving amount of a solar heating system was determined by many factors, including the types and performance parameters of the solar collector as well as the solar collector area and the local meteorological parameters. The annual energy saving amount can be calculated by the following equation:

$$\Delta Q = A_c J_t (1 - \eta_{cd}) \eta_c, \quad (20)$$

where ΔQ is the annual energy-saving amount, MJ; Ac is the area of the solar collector, m^2; J_t is the annual solar radiation projecting onto the surface of the solar collector, MJ/m^2; η_{cd} is the heat loss rate of the pipeline and water tank; η_c is the collector efficiency. In this study, the solar collector area was 860 m^2. According to GB 50495-2009 [63], the J_t in Xi'an region was 2752 MJ/m^2, η_{cd} and η_c were 25% and 75%, respectively. Thus, the annual energy-saving amount of the proposed combined SAHP system was 1,318,218 MJ by Equation (20).

In addition, the cost-saving amount of the system was also analyzed. According to [63], the annual cost-saving amount could be obtained by the following equation:

$$M_i = C_i \Delta Q, \tag{21}$$

where M_i is the annual cost-saving amount, CNY; C_i is the heat pricing of the conventional energy, CNY/MJ, which is expressed as:

$$C_i = C_i' / (q \cdot Eff), \tag{22}$$

where C_i' is the conventional energy price, CNY/kg; q is the calorific value of the conventional energy, MJ/kg; Eff is the heating efficiency of the devices with conventional energy. Generally, the coal price in China was about 450 CNY/ton and the calorific value of the standard coal was 29.308 MJ/kg. The thermal efficiency of boilers was 75%. Thus, the value of C_i could be obtained by Equation (22), which is 0.02 CNY/MJ. Consequently, the value of M_i could be obtained by Equation (21), which is 26,363 CNY.

In addition, the annual electric charges of the three systems were calculated. The annual electricity cost was taken as the evaluation index for economic comparison of the three systems. According to Figure 12, the annual energy consumption of each system could be obtained, in which the energy consumption of the serial, parallel and the proposed combined systems was 325,000, 240,278, and 188,889 kW·h, respectively. Considering that the electric price in Shaanxi region was about 0.73 CNY/kW·h, it could be obtained that the electric cost of the serial, parallel and the proposed combined systems was 237,250, 175,402, and 137,889 CNY, respectively, indicating the obvious advantage of the combined system on energy conservation. The result also suggested that the proposed combined system was more suitable for year-round operation.

5. Conclusions

In this study, a combined SAHP system that could operate in the serial mode or parallel mode was proposed. The performance of the proposed system was investigated and compared with the conventional serial and parallel systems in detail using TRNSYS simulation, which was validated through experimental measurement. The results suggested that during winter condition, the serial mode exhibited a better performance than the parallel mode; in contrast, during the summer and transition season conditions, the parallel mode had a performance advantage compared to the serial mode. Thus, the proposed system should operate in different modes corresponding to different weather conditions. Based on the mode switching method obtained by analyzing the heat balance equations, the annual performance of three different SHAP systems was comparatively evaluated. The results showed that compared to the serial and parallel systems, the proposed combined system had an obvious advantage on energy efficiency, in which the annual average COP of the proposed system was 5.7, while those of the serial and the parallel systems were 3.3 and 4.3, respectively. The finding in this study indicated the necessity and rationality of the proposed system, which could be used for actual practical engineering design.

Supplementary Materials: The following are available online at http://www.mdpi.com/1996-1073/12/13/2515/s1, Figure S1: TRNSYS model of the combined SAHP system.

Author Contributions: Conceptualization, F.W.; Data curation, Y.Z.; Formal analysis, Y.Z.; Funding acquisition, L.L. and P.T.; Investigation, C.H. and S.L.; Software, Z.W.; Writing—original draft, C.H.

Funding: The work described in this paper was supported by National Natural Science Foundation of China (Grant Nos. 51674188, 51874229, 51504182), a Scientific Research Program funded by Xi'an Science and Technology Bureau (Grand No. 201805036YD14CG20(5)), a Postdoctoral Innovative Talents Support Program from China Post-doctoral Science Foundation (BX20190280), a Shaanxi Innovative Talents Cultivate Program-New-star Plan of Science and Technology (No. 2018KJXX-083), and a Natural Science Basic Research Plan of Shaanxi Province of China (No. 2015JQ5187).

Acknowledgments: We would like to express our gratitude to Yanan Wang for her assistance.

Conflicts of Interest: The authors declare no conflict of interest.

Nomenclature

ASHP	air source heat pump
CSWT	consumer side water tank
HSWT	heat storage water tank
SAHP	solar assisted heat pump
WSHP	water source heat pump
A_c	area of the solar collector, m^2
A_s	heat exchange area of HSWT, m^2
A_w	surface area of the exterior wall, m^2
C_i	conventional energy heating price in the year of system design, CNY/MJ
C_i'	systematic assessment of conventional energy prices, CNY/kg
COP_a	COP of ASHP
COP_s	COP of WSHP
Eff	efficiency of conventional energy heating devices
F_r	heat removal factor
I	solar radiation, $kJ \cdot m^{-2} \cdot h^{-1}$
I_c	average daily solar radiation in the coldest month, $kJ \cdot m^{-2} \cdot d^{-1}$
J_t	annual solar radiation on the surface of solar collector, MJ/m^2
K_1	heat transfer coefficient of the plate to environment, $kW \cdot m^{-2} \cdot °C^{-1}$
K_s	heat transfer coefficient of HSWT, $kW \cdot m^{-2} \cdot °C^{-1}$
$(mC_p)_s$	heat capacity of water, $kJ \cdot °C^{-1} \cdot s^{-1}$
mC_p	heat capacity of the heating medium, $kJ \cdot °C^{-1} \cdot s^{-1}$
M_i	simple annual energy saving cost, CNY
q	calorific value of conventional energy, MJ/kg
$\underline{Q}$	heating capacity of CSWT for serial mode, kW
$\overline{Q}$	heating capacity of CSWT for parallel mode, kW
$\underline{Q_C}$	heat transfer rate of WSHP evaporator, kW
$\overline{Q_c}$	heat transfer rate of ASHP evaporator, kW
$\underline{Q_k}$	heat transfer rate of WSHP condenser, kW
$\overline{Q_k}$	heat transfer capacity of ASHP condenser, kW
Q_s	daily heat capacity, kW
$\underline{Q_u}$	heat collection the solar collector, kW
$\overline{Q_u}$	collecting heat of the solar collector, kW
ΔQ	annual energy-saving amount, MJ
T_a	ambient temperature, °C
T_{ca}	average water temperature of the solar collector, °C
T_{ci}	inlet water temperature of the collector, °C
T_{co}	outlet water temperature of the solar collector, °C
T_{sm}	average water temperature in HSWT, °C
V	volume of the HSWT, m^3
$\underline{W}$	compressor power of WSHP, kW
$\overline{W}$	compressor power of ASHP, kW
$(\rho c)_w$	volumetric heat capacity of the heating medium, $kJ \cdot m^{-3} \cdot °C^{-1}$
$\tau\alpha$	product of the transmittance and absorption rates of the plate

η_c	collector efficiency
η_{cd}	heat loss rate of pipeline and water tank
η_s	heat loss rate of heating medium
Δt	temperature difference, °C
$\delta T_s/\delta\tau$	water temperature change rate, °C

References

1. Zeng, R.; Wang, X.; Di, H.; Jiang, F.; Zhang, Y. New concepts and approach for developing energy efficient buildings: Ideal specific heat for building internal thermal mass. *Energy Build.* **2011**, *43*, 1081–1090. [CrossRef]
2. Bellos, E.; Tzivanidis, C.; Moschos, K.; Antonopoulos, K.A. Energetic and financial evaluation of solar assisted heat pump space heating systems. *Energy Convers. Manag.* **2016**, *120*, 306–319. [CrossRef]
3. Huang, Y.; Niu, J.; Chung, T. Study on performance of energy-efficient retrofitting measures on commercial building external walls in cooling-dominant cities. *Appl. Energy* **2013**, *103*, 97–108. [CrossRef]
4. Tzivanidis, C.; Bellos, E.; Mitsopoulos, G.; Antonopoulos, K.A.; Delis, A. Energetic and financial evaluation of a solar assisted heat pump heating system with other usual heating systems in Athens. *Appl. Therm. Eng.* **2016**, *106*, 87–97. [CrossRef]
5. Nozik, A.J. Photoelectrochemistry: Applications to Solar Energy Conversion. *Ann. Rev. Phys. Chem.* **2003**, 29189–29222. [CrossRef]
6. Lewis, N.S. Toward cost-effective solar energy use. *Science* **2007**, *315*, 798–801. [CrossRef] [PubMed]
7. Li, B. Integration of Solar Systems with Heat Pumps and Other Technologies. In *Handbook of Energy Systems in Green Buildings*; Wang, R., Zhai, X., Eds.; Springer: Berlin/Heidelberg, Germany, 2017; pp. 1372–1407.
8. Jordan, R.C.; Threlkeld, J.L. Design and economics of solar energy heat pump system. *Heat. Piping Air Cond.* **1954**, *26*, 122–130.
9. Hawlader, M.N.A.; Chou, S.K.; Ullah, M.Z. The performance of a solar assisted heat pump water heating system. *Appl. Therm. Eng.* **2001**, *21*, 1049–1065. [CrossRef]
10. Huang, B.J.; Lee, C.P. Long-term performance of solar-assisted heat pump water heater. *Renew. Energy* **2004**, *29*, 633–639. [CrossRef]
11. Hepbasli, A.; Kalinci, Y. A review of heat pump water heating systems. *Renew. Sustain. Energy Rev.* **2009**, *13*, 1211–1229. [CrossRef]
12. Sun, X.; Dai, Y.; Novakovic, V.; Wu, J.; Wang, R. Performance Comparison of Direct Expansion Solar-assisted Heat Pump and Conventional Air Source Heat Pump for Domestic Hot Water. *Energy Procedia* **2015**, *70*, 394–401. [CrossRef]
13. Liu, H.; Jiang, Y.; Yao, Y. The field test and optimization of a solar assisted heat pump system for space heating in extremely cold area. *Sustain. Cities Soc.* **2014**, *13*, 97–104. [CrossRef]
14. Yang, W.; Zhu, J.; Shi, M.; Chen, Z. Numerical Simulation of the Performance of a Solar-Assisted Heat Pump Heating System. *Procedia Environ. Sci.* **2011**, *11*, 790–797. [CrossRef]
15. Cabrol, L.; Rowley, P. Towards low carbon homes—A simulation analysis of building-integrated air-source heat pump systems. *Energy Build.* **2012**, *48*, 127–136. [CrossRef]
16. Molinaroli, L.; Joppolo, C.M.; De Antonellis, S. Numerical Analysis of the Use of R-407C in Direct Expansion Solar Assisted Heat Pump. *Energy Procedia* **2014**, *48*, 938–945. [CrossRef]
17. Wang, Z.; Guo, P.; Zhang, H.; Yang, W.; Mei, S. Comprehensive review on the development of SAHP for domestic hot water. *Renew. Sustain. Energy Rev.* **2017**, *72*, 871–881. [CrossRef]
18. Morrison, G.L.; Anderson, T.; Behnia, M. Seasonal performance rating of heat pump water heaters. *Sol. Energy* **2004**, *76*, 147–152. [CrossRef]
19. Lerch, W.; Heinz, A.; Heimrath, R. Direct use of solar energy as heat source for a heat pump in comparison to a conventional parallel solar air heat pump system. *Energy Build.* **2015**, *100*, 34–42. [CrossRef]
20. Tagliafico, L.A.; Scarpa, F.; Valsuani, F. Direct expansion solar assisted heat pumps—A clean steady state approach for overall performance analysis. *Appl. Therm. Eng.* **2014**, *66*, 216–226. [CrossRef]
21. Li, H.; Sun, L.; Zhang, Y. Performance investigation of a combined solar thermal heat pump heating system. *Appl. Therm. Eng.* **2014**, *71*, 460–468. [CrossRef]
22. Zhao, Z.; Zhang, Y.; Mi, H.; Zhou, Y.; Zhang, Y. Experimental Research of a Water-Source Heat Pump Water Heater System. *Energies* **2018**, *11*, 1205. [CrossRef]

23. Ruschenburg, J.; Herkel, S.; Henning, H.-M. A statistical analysis on market-available solar thermal heat pump systems. *Sol. Energy* **2013**, *95*, 79–89. [CrossRef]
24. Huan, C.; Wang, F.; Li, S.; Zhao, Y.; Liu, L.; Wang, Z.; Ji, C. A performance comparison of serial and parallel solar-assisted heat pump heating systems in Xi'an, China. *Energy Sci. Eng.* **2019**, *00*, 1–15. [CrossRef]
25. Bakirci, K.; Yuksel, B. Experimental thermal performance of a solar source heat-pump system for residential heating in cold climate region. *Appl. Therm. Eng.* **2011**, *31*, 1508–1518. [CrossRef]
26. Urchueguía, J.F.; Zacarés, M.; Corberán, J.M.; Montero, Á.; Martos, J.; Witte, H. Comparison between the energy performance of a ground coupled water to water heat pump system and an air to water heat pump system for heating and cooling in typical conditions of the European Mediterranean coast. *Energy Convers. Manag.* **2008**, *49*, 2917–2923. [CrossRef]
27. Gao, L.; Dougal, R.A.; Liu, S.; Iotova, A.P. Parallel-Connected Solar PV System to Address Partial and Rapidly Fluctuating Shadow Conditions. *IEEE Trans. Ind. Electron.* **2009**, *56*, 1548–1556.
28. Liang, C.; Zhang, X.; Li, X.; Zhu, X. Study on the performance of a solar assisted air source heat pump system for building heating. *Energy Build.* **2011**, *43*, 2188–2196. [CrossRef]
29. Touchie, M.F.; Pressnail, K.D. Testing and simulation of a low-temperature air-source heat pump operating in a thermal buffer zone. *Energy Build.* **2014**, *75*, 149–159. [CrossRef]
30. Dikici, A.; Akbulut, A. Performance characteristics and energy–exergy analysis of solar-assisted heat pump system. *Build. Environ.* **2008**, *43*, 1961–1972. [CrossRef]
31. Li, H.; Yang, H. Study on performance of solar assisted air source heat pump systems for hot water production in Hong Kong. *Appl. Energy* **2010**, *87*, 2818–2825. [CrossRef]
32. Bellos, E.; Tzivanidis, C. Energetic and financial sustainability of solar assisted heat pump heating systems in Europe. *Sustain. Cities Soc.* **2017**, *33*, 70–84. [CrossRef]
33. Moreno-Rodríguez, A.; González-Gil, A.; Izquierdo, M.; Garcia-Hernando, N. Theoretical model and experimental validation of a direct-expansion solar assisted heat pump for domestic hot water applications. *Energy* **2012**, *45*, 704–715. [CrossRef]
34. Banister, C.J.; Collins, M.R. Development and performance of a dual tank solar-assisted heat pump system. *Appl. Energy* **2015**, *149*, 125–132. [CrossRef]
35. Aye, L.; Charters, W.W.S.; Chaichana, C. Solar heat pump systems for domestic hot water. *Sol. Energy* **2002**, *73*, 169–175. [CrossRef]
36. Chaturvedi, S.K.; Gagrani, V.D.; Abdel-Salam, T.M. Solar-assisted heat pump—A sustainable system for low-temperature water heating applications. *Energy Convers. Manag.* **2014**, *77*, 550–557. [CrossRef]
37. Shan, P.; Lai, X. Influence of CT scanning parameters on rock and soil images. *J. Vis. Commun. Image Represent* **2019**, *58*, 642–650. [CrossRef]
38. Liu, L.; Xin, J.; Feng, Y.; Zhang, B.; Song, K. Effect of the cement-tailing ratio on the hydration products and microstructure characteristics of cemented paste backfill. *Arab. J. Sci. Eng.* **2019**. [CrossRef]
39. Liu, L.; Zhu, C.; Qi, C.; Zhang, B.; Song, K. A microstructural hydration model for cemented paste backfill considering internal sulfate attacks. *Constr. Build. Mater.* **2019**, *211*, 99–108. [CrossRef]
40. Qi, C.; Liu, L.; He, J.; Chen, Q.; Yu, L.; Liu, P. Understanding Cement Hydration of Cemented Paste Backfill: DFT Study of Water Adsorption on Tricalcium Silicate (111) Surface. *Minerals* **2019**, *9*, 202. [CrossRef]
41. Sabiha, M.A.; Saidur, R.; Mekhilef, S.; Mahian, O. Progress and latest developments of evacuated tube solar collectors. *Renew. Sustain. Energy Rev.* **2015**, *51*, 1038–1054. [CrossRef]
42. Qi, Q.M.; Wang, X.Z. *Meteorological Data Set for China's Building Thermal Environment Analysis*, 1st ed.; China Building Industry Press: Beijing, China, 2005. (In Chinese)
43. Ito, S.; Miura, N.; Wang, K. Performance of a heat pump using direct expansion solar collectors/evaporators. *Sol. Energy* **1999**, *65*, 189–196. [CrossRef]
44. Ito, S.; Miura, N.; Takano, Y. Studies of Heat Pumps Using Direct Expansion Type Solar Collectors. *J. Sol. Energy Eng.* **2005**, *127*, 60–64. [CrossRef]
45. Kuang, Y.; Wang, R.; Yu, L. Experimental study of solar assisted heat pump(SAHP) system for heat supply. *Acta Energiae Sol. Sin.* **2002**, *4*, 408–413. (In Chinese)
46. Zhang, X.; Yu, L.; Kuang, Y. Measurement Error Analysis of Solar Assisted Heat Pump System. *Energy Conserv. Technol.* **2006**, *4*, 316–320. (In Chinese)
47. Li, S.; Wang, H.; Meng, X.; Wei, X. Comparative study on the performance of a new solar air collector with different surface shapes. *Appl. Therm. Eng.* **2017**, *114*, 639–644. [CrossRef]

48. Suppiah, S.; Kutchcoskie, K.J.; Balakrishnan, P.V.; Chuang, K.T. Dissolved oxygen removal by combination with hydrogen using wetproofed catalysts. *Can. J. Chem. Eng.* **2010**, *66*, 849–857. [CrossRef]
49. Schmidt, T.; Mangold, D.; Müller-Steinhagen, H. Central solar heating plants with seasonal storage in Germany. *Sol. Energy* **1997**, *76*, 165–174. [CrossRef]
50. Badescu, V.; Staicovici, M.D. Renewable energy for passive house heating: Model of the active solar heating system. *Energy Build.* **2006**, *38*, 129–141. [CrossRef]
51. Ji, Y.; Duan, M. Operation modes of solar-assisted ground-source heat pump system in transition season. *Heat. Vent. Air Cond.* **2017**, *47*, 127–131. (In Chinese)
52. Shunroku, T. *Solar Cooling and Heating*, 1st ed.; China Building Industry Press: Beijing, China, 1982.
53. Jiang, L.Q.; Lou, J.; Jiang, J.L. Study on the selection of the parallel pattern solar heat pumps in water heating system. *Water Watstewater Eng.* **2008**, *9*, 89–91. (In Chinese)
54. Liu, L.; Yang, P.; Qi, C.; Zhang, B.; Guo, L.; Song, K. An experimental study on the early-age hydration kinetics of cemented paste backfill. *Constr. Build. Mater.* **2019**, *212*, 283–294. [CrossRef]
55. Zhao, Y.; Zhang, Z.; Ji, C.; Liu, L.; Zhang, B.; Huan, C. Characterization of particulate matter from heating and cooling several edible oils. *Build. Environ.* **2019**, *152*, 204–213. [CrossRef]
56. Moffat, R.J. Describing the uncertainties in experimental results. *Exp. Therm. Fluid Sci.* **1988**, *1*, 3–17. [CrossRef]
57. Ayompe, L.M.; Duffy, A.; McCormack, S.J.; Conlon, M. Validated TRNSYS model for forced circulation solar water heating systems with flat plate and heat pipe evacuated tube collectors. *Appl. Therm. Eng.* **2011**, *31*, 1536–1542. [CrossRef]
58. Haller, M.Y.; Bertram, E.; Dott, R.; Afjei, T.; Ochs, F.; Hadorn, J.-C. Review of Component Models for the Simulation of Combined Solar and Heat Pump Heating Systems. *Energy Procedia* **2012**, *30*, 611–622. [CrossRef]
59. Bellos, E.; Tzivanidis, C.; Delis, A.; Antonopoulos, K.A. Comparison of a Solar-Driven Heat Pump Heating System with Other Typical Heating Systems with TRNSYS. In Proceedings of the 28th International Conference on Efficiency, Cost, Optimization, Simulation and Environmental Impact of Energy Systems, Pau, France, 30 June–3 July 2015.
60. Rao, K. A method for obtaining correction coefficient of incidence angle of evacuated collector. *Acta Energiae Sol. Sin.* **2009**, *30*, 1163–1167. (In Chinese)
61. Zhang, X.M.; Jia, L.M.; Liang, Y.F.; Liu, F.X. Principle characteristics and influence factors of ASHP. *J. Hebei Inst. Archit. Sci. Technol.* **2002**, *1*, 18–21. (In Chinese)
62. Zhang, X.; Lan, G.; Du, Y.; Fei, X. Equipment Energy Balance in Solar Energy Heat Pump System. *Build. Energy Environ.* **2000**, *19*, 23–25. (In Chinese)
63. China, Ministry of Housing and Urban-Rural Construction. *Tecnical Code for Solar Heating System*; China Architecture & Building Press: Beijing, China, 2009; Volume GB 50495-2009, p. 77. (In Chinese)